

Solution Rheology of a Strongly Charged Polyelectrolyte in Good Solvent

Shichen Dou and Ralph H. Colby*

Materials Science and Engineering, The Pennsylvania State University, University Park, Pennsylvania 16802

Received January 21, 2008; Revised Manuscript Received April 28, 2008

ABSTRACT: Solution rheology of poly(2-vinylpyridine) and a random copolymer of 60% *N*-methyl-2-vinylpyridinium iodide and 40% 2-vinylpyridine in *N*-methylformamide (NMF) was studied over wide ranges of concentration. The fraction of monomers bearing an effective charge $f = 0.31$ of these copolymers was measured using dielectric spectroscopy. This low fraction of effectively charged monomers suggests that the polyion disrupts the hydrogen-bonding alignment of NMF that makes the dielectric constant of the pure solvent anomalously large. NMF is a good solvent for neutral poly(2-vinylpyridine) but has a significant quantity of ionic impurities even when freshly distilled. The specific viscosity and relaxation time of dilute and semidilute unentangled solutions exhibit the scaling with concentration expected by theory if $c_s \approx 1$ mM residual salt is present, identified from the change in slope of viscosity–concentration power laws from 5/4 to 1/2 at concentration $c = 2c_s/f = 9.5 \times 10^{-3}$ M (moles of monomer per liter). The specific viscosity data obey the Fuoss law in the semidilute unentangled regime for $c > 2c_s/f$, where there are more free counterions than residual salt ions. The correlation length measured by the peak in small-angle X-ray scattering agrees quantitatively with that obtained from the viscosity of semidilute unentangled solutions with $c > 2c_s/f$, using the scaling model.

Introduction

Polyelectrolyte solution rheology has received considerable attention^{1–17} owing to the pragmatic utility for aqueous coatings. Polyelectrolytes boost viscosity more effectively than neutral polymers of the same molar mass but simultaneously make the viscosity (and elastic character) sensitive to salt concentration. Polyelectrolyte molar mass, effective charge, concentration, and added salt concentration are all recognized to impact polyelectrolyte solution rheology.¹³ Another important factor is the solvent quality, defined for polyelectrolytes by the interaction of the neutral counterpart polymer with the same solvent. If the neutral version of the polyelectrolyte has little or no interaction with the solvent, excluded volume swells the neutral polymer significantly beyond its ideal size (so-called good solvent), and the polyelectrolyte on its smallest scales is locally swollen by excluded volume as well.^{13,18,19} *N*-Methylformamide (NMF) is a good solvent for the neutral parent poly(2-vinylpyridine) (P2VP), making the random copolymer of 40% 2-vinylpyridine and 60% *N*-methyl-2-vinylpyridinium iodide (PMVP-I) have swollen electrostatic blobs, corresponding to the good solvent case of the polyelectrolyte scaling theory.^{13,18} NMF also has a very large dielectric constant, making the polyelectrolyte strongly charged.

However, NMF has high conductivity (16.2 $\mu\text{S}/\text{cm}$ at 25 °C after careful distillation), meaning that concentrations of ionic contaminants are significant in NMF. This is analogous to aqueous solutions exposed to air, within which carbon dioxide dissolves and forms carbonic acid^{7,14,20} with a concentration of roughly 4×10^{-6} M and similar high conductivity (10 $\mu\text{S}/\text{cm}$ at 25 °C) from this residual salt. This salt contamination in NMF effectively places low polymer concentrations in the high-salt limit (with more salt ions than free counterions)¹³ while high polymer concentrations will correspond to the low salt limit. The vast majority of experimental studies of polyelectrolyte solution rheology have been in water, although some studies in polar organic solvents have been reported.^{6,17,21,22}

NMF solutions of partially quaternized P2VP provide a good test of scaling theory¹³ for polyelectrolyte solution rheology in

good solvent, for both the high salt and low salt limits. For this reason, we first briefly review the scaling predictions in good solvent before discussing our experimental data.

Background Theory

The Bjerrum length l_B is the scale at which the Coulomb energy of two charges equals the thermal energy kT

$$l_B = e^2/\epsilon kT$$

where e is the elementary charge and ϵ is the solvent dielectric constant. At 25 °C, water has $\epsilon = 78$ and $l_B = 7.1$ Å, whereas NMF has $\epsilon = 182$ and $l_B = 3.1$ Å. According to the Oosawa/Manning counterion condensation theory,^{23–25} no condensation occurs (all counterions are free, meaning that the fraction of effectively charged monomers f equals the fraction of monomers bearing a charged group α) if the local charge spacing along the chain exceeds the Bjerrum length. However, if the local conformation of the polymer makes the distance between charges along the chain smaller than the Bjerrum length, counterions condense on the chain to lower the charge repulsion until the distance between effective charges equals the Bjerrum length. Such condensed counterions no longer contribute to the counterion activity or the conductivity of the solution, but do contribute to the polarizability.²⁶ If correct, the condensation model could determine the fraction f of monomers on the chain bearing an effective charge. However, the detailed local conformation of the polyelectrolyte and the precise placement of randomly charged monomers along the chain are not known *a priori*, so in practice f must be measured, typically using a counterion selective electrode,¹⁶ osmotic pressure,^{13,27} or from dielectric/conductometric measurements.²⁶ For strongly charged polyelectrolytes in polar solvents, the effective fraction of charged monomers f is expected to be significantly larger than zero, smaller than the chemical fraction of quaternized monomers, and independent of concentration.¹⁸

The local conformation of a polyelectrolyte chain in solution is determined by charge repulsion and interaction of the monomers with solvent.^{13,18,19} For dilute solution in a good solvent, charge repulsion stretches the chain into a directed random walk of electrostatic blobs (of size ξ_e containing g_e

* To whom correspondence should be addressed. E-mail: rhc@plmsc.psu.edu.

monomers) within which the cumulative electrostatic repulsion equals the thermal energy.

$$\frac{(fg_e e)^2}{\epsilon \xi_e} = kT \quad (1)$$

Inside the electrostatic blobs the chain conformation is not affected by electrostatics and hence is a self-avoiding walk in good solvent

$$\xi_e = b g_e^{3/5} \quad (2)$$

where b is the monomer size, which for vinyl monomers is $b = 2.5 \text{ \AA}$.²⁸

The above two equations can be solved for ξ_e and g_e .

$$\xi_e = b^{10/7} l_B^{-3/7} f^{-6/7} \quad \text{and} \quad g_e = (b/l_B)^{5/7} f^{-10/7} \quad (3)$$

The contour length of the chain of electrostatic blobs is

$$L = \xi_e \frac{N}{g_e} = bN \left(\frac{l_B}{b} \right)^{2/7} f^{4/7} = \frac{bN}{B} \quad (4)$$

where the last relation effectively defines the stretching parameter B as the ratio of the maximum possible contour length bN and the actual contour length of the chain of electrostatic blobs. The overlap concentration in the high salt limit is¹³

$$c^* = \left(\frac{B}{b} \right)^{6/5} N^{-4/5} (2c_s/f)^{3/5} \quad (5)$$

where c_s is the number density of fully dissociated univalent salt molecules dissociated in solution, and it is important to point out that all polymer concentrations in this paper are monomer number densities. In dilute solution the specific viscosity $\eta_{sp} = (\eta - \eta_s)/\eta_s$, where η is the (zero shear rate) solution viscosity and η_s is the solvent viscosity, is predicted to be^{13,19}

$$\eta_{sp} = \frac{c}{c^*} \quad \text{for } c < c^* \quad (6)$$

making the intrinsic viscosity $[\eta] = \lim_{c \rightarrow 0} (\eta_{sp}/c) = 1/c^*$. The overlap concentration in this work is experimentally estimated as the concentration at which the specific viscosity is unity. However, both $[\eta]$ and c^* for high molar mass polyelectrolytes in NMF correspond to the high salt limit. This limit is defined as having more salt ions than free counterions¹³ ($2c_s > fc$). For our polyelectrolyte in NMF solution, the border between the low salt and high salt solutions ($c = 2c_s/f$) is above c^* in the semidilute unentangled solution. For this reason, both high salt and low salt semidilute unentangled solution scaling predictions are discussed (and observed).

Above the overlap concentration, charge repulsion is partially screened by other chains (and their free counterions). Such semidilute solutions are characterized by a correlation length^{13,19,29} ξ , which is the typical distance to the nearest chain.

$$\xi = \left(\frac{B}{cb} \right)^{1/2} \left[1 + \frac{2c_s}{fc} \right]^{1/4} \quad \text{for } c > c^* \quad (7)$$

The contour length is still L (given by eq 4), but the root-mean-square end-to-end distance R is smaller than in dilute solution, since the chain is a random walk on its largest scales.^{13,18}

$$R = \left(\frac{b}{cB} \right)^{1/4} N^{1/2} \left[1 + \frac{2c_s}{fc} \right]^{-1/8} \quad \text{for } c > c^* \quad (8)$$

The scaling model¹³ predicts the chain in semidilute unentangled solutions relaxes by Rouse motion,²⁹ with relaxation time

$$\tau = \frac{\tau_0 N^2}{(cb^3 B^3)^{1/2}} \left[1 + \frac{2c_s}{fc} \right]^{-3/4} \quad \text{for } c^* < c < c_e \quad (9)$$

where $\tau_0 = \eta_s b^3/kT$ is the relaxation time of a monomer²⁹ and c_e is the concentration at which polymer chains in solution start to show entanglement effects. The terminal modulus G is predicted to be kT per chain^{13,29} below c_e .

$$G = \frac{ckT}{N} \quad \text{for } c < c_e \quad (10)$$

The specific viscosity is the product of relaxation time and terminal modulus divided by solvent viscosity.²⁹

$$\eta_{sp} = \frac{\tau G}{\eta_s} = \left(\frac{cb^3}{B^3} \right)^{1/2} N \left[1 + \frac{2c_s}{fc} \right]^{-3/4} \quad \text{for } c^* < c < c_e \quad (11)$$

The low salt limit ($c > 2c_s/f$) of this scaling prediction is the same as the empirical Fuoss law.¹⁻³ Equations 9–11 quantitatively describe the rheology of semidilute unentangled aqueous polyelectrolyte solutions in both the low salt and high salt limits (and their crossover).^{14,16} The concentration $2c_s/f$ separating the high salt and low salt regimes is easily identified as a change in exponent from 5/4 to 1/2 in a plot of the concentration dependence of specific viscosity on logarithmic scales, based on eq 11.

The entanglement concentration in the low salt limit (assuming $c_e > 2c_s/f$) is expected to be proportional to the overlap concentration in the low salt limit.¹³

$$c_e \sim \frac{B^3}{b^3 N^2} = b^{-3} N^{-2} \left(\frac{b}{l_B} \right)^{6/7} f^{-12/7} \quad (12)$$

For $c > c_e$, there is a semidilute entangled regime of polyelectrolyte solution rheology.¹³ The relaxation time is predicted to be *independent of concentration*. The terminal modulus is predicted to scale as the 3/2 power of concentration, and the specific viscosity is then also predicted to scale as the 3/2 power of concentration.¹³ Comparing these concentration exponents with those in eqs 9–11, it is evident that the entanglement concentration is easily identified by changes in slope in plots on logarithmic scales.

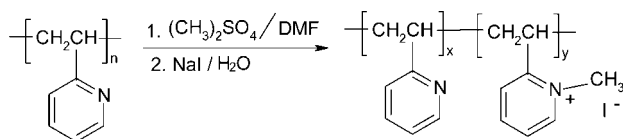
Experimental Section

Solvent. *N*-Methylformamide (NMF; bp 198–199 °C, mp –4 °C, density 1.011 g/mL, ACS reagent grade ≥99.0% purity) was purchased from Aldrich. NMF was soaked in 4 Å active molecular sieves for over 48 h, stirred, filtered, and then distilled under reduced pressure (<100 mTorr under argon) at 70–80 °C. The distillation procedure was repeated twice for the middle fraction to obtain purified NMF with conductivity of 16.2 μS/cm.

NMF is a *N*-monoalkylated amide solvent with very high dielectric constant ($\epsilon = 182$ at 25 °C) and shows both acidic and basic character by donating or accepting a proton. Oncescu et al.³⁰ reported that the conductivity of NMF at 25 °C is 0.7 μS/cm after being carefully purified. Sehgal and Seery³¹ indicated that the concentration of residual salt in NMF “as received” is larger than 0.02 M and the conductivity of NMF “as received” is 509 μS/cm, but the conductivity of NMF can be lowered to 6.3 μS/cm by stirring with ion-exchange resin and molecular sieves for 2.5 h. NMF is a strongly hygroscopic solvent; it can absorb water and carbon dioxide and then slowly hydrolyze to form ammonia, formate, and carbonate due to its molecular structure and high dielectric constant. NMF demonstrates very low pK_a (10.74) and, hence, is a powerful dissociating solvent³⁰ and acts as a protic solvent in the solvation of ions.³²

NMF has a large vapor-phase dipole moment of 3.82 D, similar to that of other alkyl amides.³³ In the liquid state at 25 °C, NMF displays very strong hydrogen bonding, with a Kirkwood correlation factor^{34,35} $g = 3.3$ and a broad dielectric relaxation centered at 1.2 GHz.³⁶ Barthel et al.³⁷ reported that the Kirkwood correlation factor

Scheme 1



of NMF is significantly larger ($g = 4.57$ at $25\text{ }^{\circ}\text{C}$) than the $g = 3.3$ reported by Cole and co-workers³⁴ from comparison of gas-phase and liquid-phase dielectric constants. NMF predominantly forms chainwise associations linked by hydrogen bonds with the single amino hydrogen, so that the adjacent molecular dipoles are almost parallel to each other, causing the large g and very high dielectric constant.

Polymer. Poly(2-vinylpyridine) (P2VP, $M_w = 1\,220\,000$ g/mol, $M_w/M_n = 1.1$, $N = 10\,500$, based on M_n) purchased from Polymer Source Inc. was used without further purification. Such a long chain polymer with narrow molecular weight distribution is ideal for testing the predictions discussed above. Anhydrous reagents dimethyl sulfate (DMS, 99%, DuPont) and sodium iodide (Aldrich, 99.5%) were used as received. *N,N*-Dimethylformamide (DMF: Aldrich, anhydrous, 99.8%) was redistilled under vacuum in the presence of sodium.

Quaternization. A random copolymer of 2-vinylpyridine and *N*-methyl-2-vinylpyridinium iodide was prepared by quaternization and ion exchange (Scheme 1). Parent dry P2VP was added into a 100 mL reactor under argon; DMF was then added to make a 10 wt % solution of the P2VP in DMF. DMS was injected into the reactor when the P2VP had fully dissolved in DMF. The reaction was kept at room temperature 24 h under argon. The quaternized polymer was precipitated into acetone, filtered, and then redissolved in 2 M NaI solution in water with at least 50-fold excess of iodide to methylpyridinium ion^{8,9} and then dialyzed against deionized water until a constant conductivity ($< 2\text{ }\mu\text{S/cm}$) of the dialyze was attained. Finally, the salt-free polyelectrolyte solution was lyophilized under vacuum, and the solid quaternized polymer was dried in a vacuum oven at $40\text{ }^{\circ}\text{C}$ to a constant mass. Dry polymer was dissolved in fresh redistilled NMF to prepare the highest concentration, and lower concentrations were prepared by serial dilution. Polymer concentration is reported in moles of monomers (the sum of both vinylpyridine and methyl vinylpyridinium iodide) per liter of solution.

The degree of quaternization of the partially quaternized polymer was determined using silver nitrate (Aldrich, 99.9%) conductometric counterion titration, calibrated with sodium chloride (Aldrich, 99.999%), as detailed in ref 17. The degree of quaternization is 60 mol %. We were unable to obtain quaternized P2VP with more than 60 mol % charged monomers, similar to the maximum quaternization extents of high molecular weight P2VP reported previously using this chemistry (55 mol % in ref 17; 70 mol % in ref 38; 82 mol % in ref 8, which also demonstrated that 100% quaternization could be achieved in roughly 30 days).

Effective Charge f . Conductivity measurements were performed with a broadband dielectric spectrometer (Novocontrol GmbH, Germany). The conductivity of fresh polyelectrolyte solutions in the concentration range from 0.01 to 10 mg/mL in a liquid cell (spacer: 0.55 mm; diameter: 20 mm) was measured at $25\text{ }^{\circ}\text{C}$, frequency range from 10^{-1} to 3×10^6 Hz, and voltage amplitude 0.1 V (ac). Conductivity was evaluated in a roughly 2 decade frequency range where the in-phase conductivity was independent of frequency (from 10^2 to 10^4 Hz at low concentrations, gradually increasing to 10^4 to 10^6 Hz at the highest concentrations studied). Higher frequencies show a relaxation from polarization of free counterions, and lower frequencies show electrode polarization effects.²⁶ Equivalent conductance $\Lambda = (\sigma - \sigma_s)/c$ was determined from the conductivity of polyelectrolyte solutions (σ), the conductivity of NMF (σ_s), and the molar concentration of monomer (c). The concentration dependence of equivalent conductance in NMF is shown in Figure 1. The equivalent conductance of the iodide counterion in NMF has been measured³⁹ to be $\lambda_c = 22.76\text{ S cm}^2/\text{mol}$. Using this value in the simple model for conductivity of

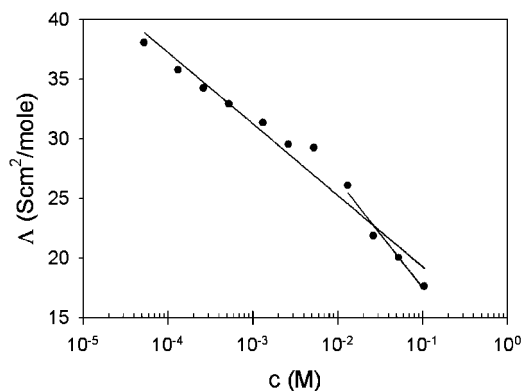


Figure 1. Concentration dependence of equivalent conductance for 60% quaternized P2VP polyelectrolyte solutions in NMF at $25\text{ }^{\circ}\text{C}$. Symbols are experimental data, and lines are fits to determine the effective charge (see text).

polyelectrolyte solutions ignoring any asymmetric field effects allows us to make a two-parameter fit of the data in Figure 1 using the following equation for equivalent conductance.^{26,40}

$$\Lambda = f \left(\lambda_c + \frac{f c \xi^2 e^2 \ln(\xi/\xi_e)}{3\pi\eta_s} \right) \quad (13)$$

Using the SAXS and rheology measures of the correlation length presented later in Figure 6, $c\xi^2 = 1450\text{ }\text{\AA}^2\text{ mol/L} = 8.7 \times 10^8\text{ cm}^{-1}$. The solvent viscosity of NMF is 1.74 mPa s at $25\text{ }^{\circ}\text{C}$, making $c\xi^2 e^2/(3\pi\eta_s) = 82\text{ S cm}^2/\text{mol}$. The data in Figure 1 were fit to eq 13, resulting in two parameters: the fraction of monomers bearing an effective charge f and the electrostatic blob size ξ_e . Fitting all of the data in Figure 1 yields $f = 0.25$ and $\xi_e = 8.9\text{ }\text{\AA}$. However, only the four highest concentrations have more free counterions than salt ions, thus corresponding to the low salt limit where eq 13 should apply. Using only those highest four concentrations in the fit to eq 13 yields $f = 0.31$ and $\xi_e = 32\text{ }\text{\AA}$. These latter numbers are closer to naïve expectations of large f in the high dielectric constant solvent and large electrostatic blobs in a good solvent. The chloride salts of partially quaternized P2VP in ethylene glycol (EG, another good solvent) have $f = 0.18$ (owing to lower dielectric constant of ethylene glycol) and $\xi_e = 32\text{ }\text{\AA}$ for large extents of quaternization.¹⁷ Consequently, in the good solvents NMF and EG, the swollen electrostatic blobs are quite large ($\xi_e = 32\text{ }\text{\AA}$) with $g_e \approx 70$ monomers per electrostatic blob.

Rheology. The steady shear viscosity of solutions in NMF was measured at $25\text{ }^{\circ}\text{C}$ using a Rheometrics Fluids Spectrometer (RFS-II, controlled strain) with concentric cylinder geometry, calibrated using Newtonian oils of known viscosity at $25\text{ }^{\circ}\text{C}$. All of our polyelectrolyte solutions in NMF showed appreciable shear thinning, and the apparent viscosity (η) of solutions in NMF was measured as a function of shear rate ($\dot{\gamma}$), with the data plotted in Figure 2, along with fits to the Carreau model⁴¹

$$\eta(\dot{\gamma}) = \frac{\eta(0)}{[1 + (\tau\dot{\gamma})^2]^p} \quad (14)$$

to determine the relaxation time τ and the parameter p by least-squares regression. The parameter p was found to systematically change with concentration, as seen in other studies of polyelectrolyte solution rheology, ranging from 0.05 at low concentration to 0.25 at high concentration.⁴² The relaxation time obtained by fitting the shear rate dependence of apparent viscosity to eq 14 has been shown to agree with the linear viscoelastic relaxation time of polyelectrolyte solutions,^{15,17,42} determined as the reciprocal angular frequency at which the terminal power laws of storage and loss moduli extrapolate to intersection.²⁹

Small-Angle X-ray Scattering. Measurements were performed at $25\text{ }^{\circ}\text{C}$, using a Molecular Metrology SAXS instrument with a

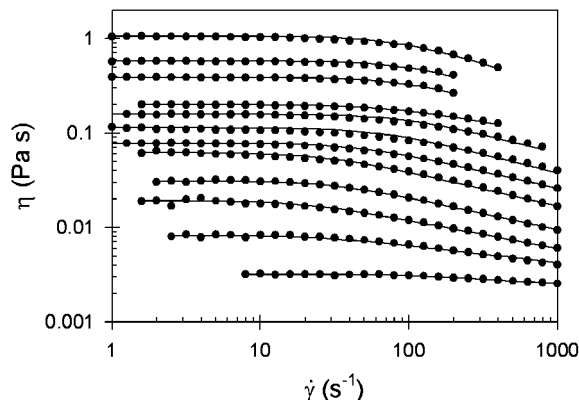


Figure 2. Shear rate dependence of apparent viscosity (open squares) and the Carreau model fits (lines) for 60PMVP-I solutions in NMF at 25 °C. Solution concentrations from top to bottom are 0.788, 0.526, 0.368, 0.210, 0.105, 0.0526, 0.0263, 0.0131, 0.00526, 0.00263, 0.00131, and 0.000526 mol/L.

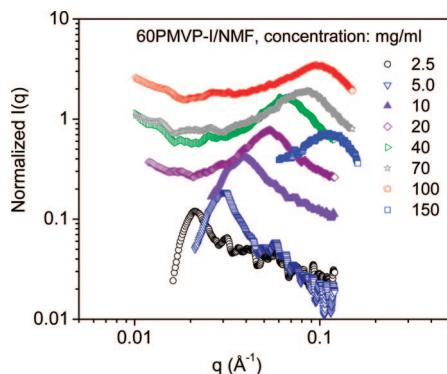


Figure 3. SAXS profiles for 60PMVP-I solutions in NMF at 25 °C in the low salt semidilute region; $I(q)$ was subtracted from the background scattering intensity and then normalized using the sample thickness, experiment time, and transmission intensity.

Cu K α radiation source (wavelength $\lambda = 1.54$ Å), a 12.5 cm \times 12.5 cm two-dimensional gas-filled wire-grid detector, and a photodiode in the beam stop to measure intensity of the transmitted beam. The distance between sample and detector is 224 cm. Liquid cells with Kapton windows were used to hold the polymer solutions for SAXS measurements. The thickness of these liquid cells is 1.2 mm (for concentrations $c < 30$ mg/mL) and 0.4 mm (for $c > 30$ mg/mL). The SAXS data are background corrected and normalized by subtracting the q -dependent scattering intensity of the background (from NMF with Kapton windows, without polymer in the same cell) from that of the sample, and then normalized by sample thickness d .

$$I(q) = \frac{1}{d} \left[\frac{I_s(q)}{t_s} \left(\frac{I_{bt} - I_{DC}}{I_{st} - I_{DC}} \right) - \frac{I_b(q)}{t_b} \right] \quad (15)$$

$I_s(q)$ is the q -dependent scattering intensity recorded for the sample in scattering time t_s , $I_b(q)$ is the q -dependent scattering intensity recorded for the background in scattering time t_b , I_{bt} is the transmitted beam intensity for the background, I_{st} is the transmitted beam intensity for the sample, and I_{DC} is the “dark current” intensity of the transmitted beam when the beam is switched off.

The normalized intensity profiles $I(q)$ from eq 15 for 60PMVP-I solutions in NMF shown in Figure 3 indicate that 60PMVP-I is highly structured in NMF solutions, exhibiting strong polyelectrolyte behavior.

Results and Discussion

1. Specific Viscosity. Specific viscosity $\eta_{sp} = (\eta - \eta_s)/\eta_s$ (where $\eta_s = 1.74$ mPa s is the viscosity of NMF at 25 °C)

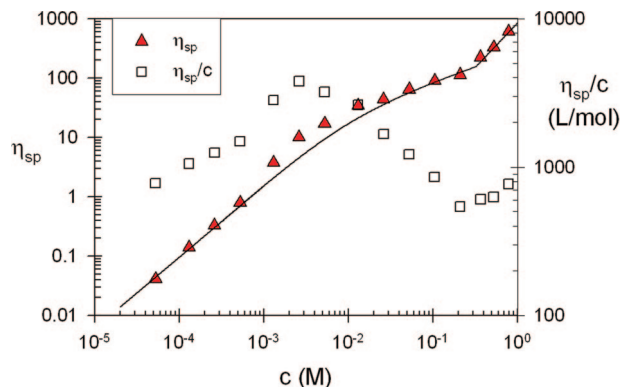


Figure 4. Concentration dependence of specific viscosity ($\eta_{sp} = (\eta - \eta_s)/\eta_s$) and reduced viscosity (η_{sp}/c) for 60PMVP-I in NMF at 25 °C.

and reduced viscosity η_{sp}/c are plotted against concentration, spanning 4 decades, in Figure 4. For dilute solutions ($c < c^* = 7.1 \times 10^{-4}$ M), the data in Figure 4 are qualitatively consistent with the scaling expected by eq 6; the apparent slope in dilute solution is 1.2. Above the overlap concentration ($c > c^*$), eq 11 describes semidilute unentangled specific viscosity, with a crossover from the high salt limit at high concentration (with slope $1/2$ for $2c_s/f \ll c < c_e$). Between c^* and c_e , the eq 11 crossover is shown as a smooth curve that is slightly lower than the data. At the entanglement concentration c_e the scaling model expects another change in slope with $\eta_{sp} \sim c^{3/2}$ for $c > c_e$. Figure 4 displays all four expected slopes, with roughly 1 decade of concentration in each regime, providing unambiguous determinations of $c_s/f = 0.0048$ M and $c_e = 0.32$ M. Figure 1 provides two estimates of f . If only conductivity data in the low salt regime are used, we conclude that $f = 0.31$, making $c_s = 1.5$ mM. If all conductivity data are used, then $f = 0.25$ and $c_s = 1.2$ mM.

Polyelectrolyte solutions in water show qualitatively similar concentration dependence of specific viscosity,^{14,15} with all four of the slopes seen in Figure 4, but in water the low salt semidilute unentangled regime persists for roughly 3 decades in concentration because the residual salt concentration is significantly smaller. Distilled water exposed to air has a residual salt level of 4×10^{-6} M from carbonic acid,^{7,14,20} with pH = 5.4 and conductivity of 10 μ S/cm. Freshly distilled NMF has a considerably higher residual salt content than distilled water, with apparent salt concentration roughly 200 \times larger than water. At first glance, the 200 \times higher salt concentration in NMF compared to water is surprising, given the fact that conductivities of these solvents are comparable. Carbonic acid in water dissociates to hydronium ion, which has 5–10 \times higher mobility than other cations owing to special proton-exchange conduction pathways. Water has 2 \times lower viscosity than NMF. Also, owing to the large dipole of 3.82 D, NMF interacts strongly with small ions,⁴³ and consequently the (unidentified) residual salt ions may well have quite low mobilities in NMF.

2. Correlation Length. The SAXS data of Figure 3 show a strong peak due to the local structure of the polyelectrolyte solutions.¹⁸ A schematic illustration of a semidilute polyelectrolyte solution in the low salt limit is given in Figure 5. Inside the electrostatic blobs (of size ξ_e) the conformation is a self-avoiding walk (in good solvent). On scales larger than ξ_e the chain is highly extended (a directed random walk) owing to charge repulsion. The same charge repulsion structures the semidilute solution with a relatively uniform distance to the nearest chain that is the correlation length ξ . Hence, charge repulsion between neighboring chains causes polyelectrolyte solutions to have a peak in their scattering function,¹⁸ and the

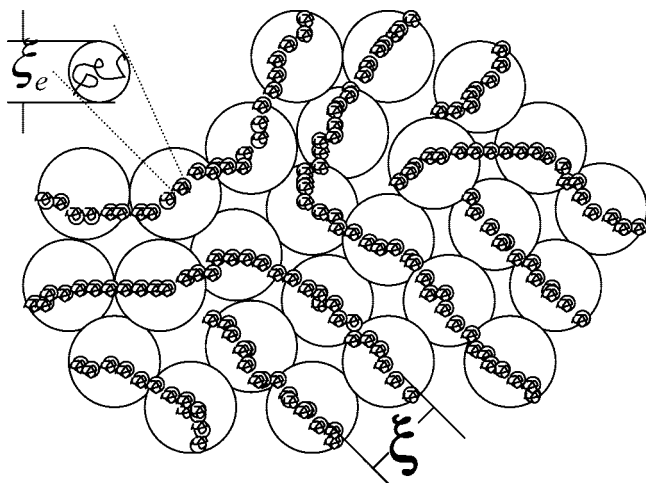


Figure 5. Schematic representation of the low salt limit for a semidilute polyelectrolyte solution in good solvent. The electrostatic blobs have self-avoiding walk conformation, and charge repulsion on larger scales simultaneously stretches the chain of electrostatic blobs locally and structures the solution so that the distance between chains is quite close to the correlation length ξ .

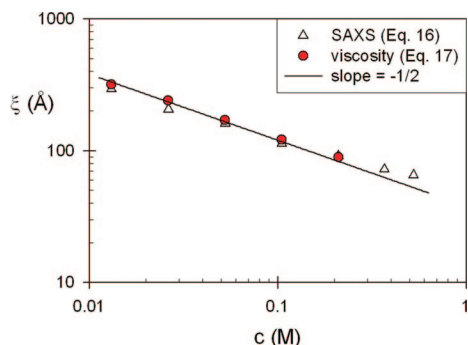


Figure 6. Concentration dependence of the correlation length ξ of 60PMVP-I in NMF determined from SAXS using eq 16 and from specific viscosity of semidilute unentangled solutions in the low-salt limit using eq 17. The power law line is eq 18.

correlation length is determined from the wavevector q_{\max} of this peak.

$$\xi = \frac{2\pi}{q_{\max}} \quad (16)$$

Combining eqs 7 and 11 gives a direct relation between specific viscosity and correlation length, valid for semidilute unentangled solutions.¹⁵

$$\xi = \left(\frac{N}{c\eta_{\text{sp}}} \right)^{1/3} \quad (17)$$

The correlation lengths calculated from SAXS peaks using eq 16 and from specific viscosity of semidilute unentangled solutions using eq 17 are compared in Figure 6. All data in Figure 6 correspond to the low salt limit, so the two methods agree very nicely, and obey the prediction of eq 7 in the low salt limit, first predicted by de Gennes et al.¹⁸

$$\xi = \sqrt{\frac{B}{bc}} \quad (18)$$

Linear regression of the data in Figure 6 yields $c\xi^2 = 1450 \text{ Å}^2 \text{ mol/L}$ and with $b = 2.5 \text{ Å}$, we conclude that the stretching parameter $B = 2.2$ for 60PMVP-I in NMF at 25 °C.

3. Relaxation Time τ and Terminal Modulus G . The relaxation time τ of polyelectrolyte solutions was determined

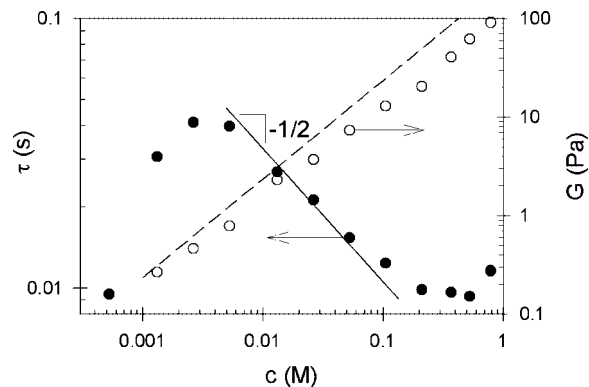


Figure 7. Concentration dependence of relaxation time determined from fitting the Carreau model (eq 14) to the shear rate dependence of apparent viscosity (filled symbols) and concentration dependence of the terminal modulus (open symbols). The solid line is the scaling expected for the relaxation time, by the low salt limit of eq 9, and the dashed line is kT per chain expected for the terminal modulus (eq 10) with no adjustable parameters for the latter.

by fitting the Carreau model (Figure 2 and eq 14) to the steady shear viscosity data. Despite semidilute unentangled solution viscosity being described by the Rouse model,^{13,29} a universal shear thinning is always observed,⁴² with longest linear viscoelastic relaxation time τ determined^{15,17,42} from fitting data to eq 14. Figure 7 plots the concentration dependences of longest relaxation time τ and terminal modulus^{13,29} $G = \eta_{\text{sp}}\eta/\tau$.

Scaling theories^{13,29} predict that the relaxation time of a polyelectrolyte solution without added salt *decreases* with increasing concentration $\tau \sim c^{-1/2}$ in the semidilute unentangled regime, based on the Rouse model and the assumption that the polyelectrolyte chain is a random walk of correlation volumes. This prediction is shown as the solid line in Figure 7 and agrees reasonably with the data in the semidilute unentangled regime.

The terminal modulus is kT per chain for $c^* < c < c_e$, in near-quantitative agreement with eq 10. For $c > c_e \approx 0.22 \text{ M}$, the terminal modulus does *not* show the scaling expected ($G \sim c^{3/2}$) for entangled polyelectrolyte solutions;¹³ instead, the terminal modulus remains slightly less than kT per chain.

4. Fraction of Monomers Bearing an Effective Charge.

The rheology is mostly consistent with a moderately charged polyelectrolyte in good solvent. The most surprising observation is that the fraction of monomers that bear an effective (not condensed) charge is so small (either $f = 0.25$ or $f = 0.31$) considering the dielectric constant $\epsilon = 182$ is so large for NMF. Figure 8 plots f as a function of the extent of quaternization α , comparing data from conductivity in ethylene glycol (EG) solutions¹⁷ and NMF solutions with the expectations of the Oosawa/Manning counterion condensation model (solid lines). In EG, the measured f agrees rather well with the Oosawa/Manning model, although the crossover from no condensation to condensation is broader than anticipated by that model. This broad crossover has been observed consistently in the polyelectrolyte solution literature, with the best examples from the work of Essafi et al.⁴⁴ However, the f values reported here in NMF solution (open circles in Figure 8) are drastically lower than the expected values. The dielectric constant $\epsilon = 182$ is so large for NMF that with 60% of the monomers quaternized we expect nearly all of the quaternized monomers to bear an effective charge, with f nearly 0.6. However, a large part of the dielectric constant of NMF comes from the Kirkwood correlations involving alignment of neighboring solvent molecules. If we divide the dielectric constant of $\epsilon = 182$ by the Kirkwood correlation factor $g = 3.3$, we get an effective dielectric constant for NMF with no alignment correlations of $\epsilon = 55$, and this leads to an Oosawa/Manning expectation of $f = 0.24$, in quite

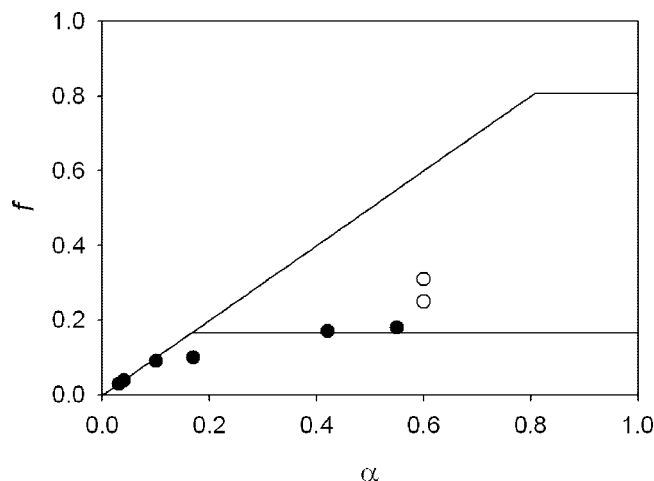


Figure 8. Observed dependence of the fraction of monomers bearing an effective charge f as a function of quaternization extent α , for partially quaternized poly(2-vinylpyridine) in ethylene glycol (filled symbols)¹⁷ and in *N*-methylformamide (open symbols). Lines are the expectations of the Oosawa/Manning condensation model^{23–25} with monomer size $b = 2.5$ Å and Bjerrum length $l_B = 15$ Å in ethylene glycol and $l_B = 3.1$ Å in NMF. Using the vapor phase dipole moment³³ of NMF without the Kirkwood correlation factor would add a horizontal line with $f = 0.24$ (not shown) which agrees nicely with the experimental f .

good agreement with the f values for polyelectrolytes in NMF reported here and elsewhere.⁴⁵ Small ions are known to compete and interfere with hydrogen bonding.⁴⁶ Perhaps near the polyelectrolyte chain the solvent correlations are disrupted by the presence of the polyion (with its strong charge) and its counterions. Such a disruption might make the effective dielectric constant determined by the measured vapor phase dipole moment of the solvent without alignment correlations.

Conclusions

Solutions of partially quaternized poly(2-vinylpyridine) in the high dielectric constant solvent NMF demonstrate the scaling predictions for concentration dependences of correlation length, specific viscosity, longest relaxation time, and terminal modulus. Despite multiple distillations, NMF solutions seem to have a very large concentration of residual salt ($c_s \approx 1$ mM) that is roughly 200 times larger than the residual salt concentration in distilled water exposed to air. This makes the low salt limit of our polyelectrolyte solutions in NMF only for monomer concentrations $c > 0.01$ M. In the range of concentration that corresponds to both the low salt limit and semidilute unentangled solution ($0.01 \text{ M} < c < 0.3 \text{ M}$) the correlation length deduced from specific viscosity agrees perfectly with the correlation length measured directly by SAXS.

In addition to the very high residual salt concentration in NMF, the fraction of monomers bearing an effective charge $f = 0.31$ is not much larger than typical values for polyelectrolytes in water. At first glance, this is surprising since the dielectric constant and vapor-phase molecular dipoles of NMF ($\epsilon = 182$; $\mu = 3.8$) are more than twice those of water ($\epsilon = 78$; $\mu = 1.8$) at 25 °C. Apparently, either the Kirkwood alignment correlations are lost for NMF in the presence of the polyion or NMF is simply less proficient than water at solvating ions. Neither scenario would be at all surprising. Iodide is known to disrupt the hydrogen-bonding alignment of NMF.⁴⁷ Indeed, the hydrogen-bonding structure of NMF is particularly sensitive to the presence of ions, as evidenced by a rapid drop in dielectric constant as electrolytes are added to NMF.⁴³

Acknowledgment. We thank the National Science Foundation, through grant DMR-0705745, for support of this research.

References and Notes

- (1) Fuoss, R. M.; Strauss, U. P. *J. Polym. Sci.* **1948**, *3*, 246.
- (2) Fuoss, R. M. *J. Polym. Sci.* **1948**, *3*, 603.
- (3) Fuoss, R. M. *Discuss. Faraday Soc.* **1951**, *11*, 125.
- (4) Eisenberg, H.; Pouyet, J. *J. Polym. Sci.* **1954**, *13*, 85.
- (5) Sakai, M.; Noda, I.; Nagasawa, M. *J. Polym. Sci., Part A-2* **1972**, *10*, 1047.
- (6) Hara, M.; Wu, J. L.; Lee, A. H. *Macromolecules* **1988**, *21*, 2214.
- (7) Cohen, J.; Priel, Z. *J. Chem. Phys.* **1988**, *88*, 7111.
- (8) Yamaguchi, M.; Yamaguchi, Y.; Matsushita, Y.; Noda, I. *Polym. J.* **1990**, *22*, 1077.
- (9) Yamaguchi, M.; Wakutsu, M.; Takahashi, Y.; Noda, I. *Macromolecules* **1992**, *25*, 470.
- (10) Yamaguchi, M.; Wakutsu, M.; Takahashi, Y.; Noda, I. *Macromolecules* **1992**, *25*, 475.
- (11) Takahashi, Y.; Hase, H.; Yamaguchi, M.; Noda, I. *J. Non-Cryst. Solids* **1994**, *172–174*, 911.
- (12) Takahashi, Y.; Iio, S.; Matsumoto, N.; Noda, I. *Polym. Int.* **1996**, *40*, 269.
- (13) Dobrynin, A. V.; Colby, R. H.; Rubinstein, M. *Macromolecules* **1995**, *28*, 1859.
- (14) Boris, D. C.; Colby, R. H. *Macromolecules* **1998**, *31*, 5746.
- (15) Krause, W. E.; Tan, J. S.; Colby, R. H. *J. Polym. Sci., Polym. Phys.* **1999**, *37*, 3429.
- (16) Konop, A. J.; Colby, R. H. *Macromolecules* **1999**, *32*, 2803.
- (17) Dou, S.; Colby, R. H. *J. Polym. Sci., Polym. Phys.* **2006**, *44*, 2001.
- (18) de Gennes, P.-G.; Pincus, P.; Velasco, R. M.; Brochard, F. *J. Phys. (Paris)* **1976**, *37*, 1461.
- (19) de Gennes, P.-G. *Scaling Concepts in Polymer Physics*; Cornell University Press: Ithaca, NY, 1979.
- (20) Shedlovsky, T.; MacInnes, D. A. *J. Am. Chem. Soc.* **1935**, *57*, 1705.
- (21) Agarwal, P. K.; Garner, R. T.; Graessley, W. W. *J. Polym. Sci., Part B: Polym. Phys.* **1987**, *25*, 2095.
- (22) Jousset, S.; Bellissent, H.; Galin, J. C. *Macromolecules* **1998**, *31*, 4520.
- (23) Oosawa, F. *J. Polym. Sci.* **1957**, *23*, 421.
- (24) Manning, G. S. *J. Chem. Phys.* **1969**, *51*, 924.
- (25) Oosawa, F. *Polyelectrolytes*; Marcel Dekker: New York, 1971.
- (26) Bordini, F.; Cametti, C.; Colby, R. H. *J. Phys.: Condens. Matter* **2004**, *16*, R1423.
- (27) Wang, L.; Bloomfield, V. A. *Macromolecules* **1990**, *23*, 804.
- (28) Fischer, K.; Schmidt, M. *Macromol. Rapid Commun.* **2001**, *22*, 787.
- (29) Rubinstein, M.; Colby, R. H. *Polymer Physics*; Oxford University Press: New York, 2003.
- (30) Oncescu, T.; Oancea, A. M.; Maeyer, L. D. *J. Phys. Chem.* **1980**, *84*, 3090.
- (31) Sehgal, A.; Seery, T. A. P. *Macromolecules* **1998**, *31*, 7340.
- (32) Parker, A. J. *J. Chem. Soc.* **1961**, 1328.
- (33) Meighan, R. M.; Cole, R. H. *J. Phys. Chem.* **1964**, *68*, 503.
- (34) Bass, S. J.; Nathan, W. I.; Meighan, R. M.; Cole, R. H. *J. Phys. Chem.* **1964**, *68*, 509.
- (35) Puranik, S. M.; Kumbharkhane, A. C.; Mehrotra, S. C. *Indian J. Chem.* **1993**, *32A*, 613.
- (36) Buchner, R.; Barthel, J. *Ber. Bunsen-Ges. Phys. Chem.* **1997**, *101*, 1509.
- (37) Barthel, J.; Buchner, R.; Wurm, B. *J. Mol. Liq.* **2002**, *98* (99), 51.
- (38) Ermi, B. D.; Amis, E. J. *Macromolecules* **1998**, *31*, 7378.
- (39) Gopal, R.; Bhatnagar, O. N. *J. Phys. Chem.* **1966**, *70*, 3007.
- (40) Colby, R. H.; Boris, D. C.; Krause, W. E.; Tan, J. S. *J. Polym. Sci., Polym. Phys.* **1997**, *35*, 2951.
- (41) Dealy, J. M.; Wissbrun, K. F. *Melt Rheology and Its Role in Plastics Processing Theory and Applications*; Kluwer Academic Publishers: Boston, 1999.
- (42) Colby, R. H.; Boris, D. C.; Krause, W. E.; Dou, S. *Rheol. Acta* **2007**, *46*, 569.
- (43) Wurm, B.; Baar, C.; Buchner, R.; Barthel, J. *J. Mol. Liq.* **2006**, *127*, 14.
- (44) Essafi, W.; LaFuma, F.; Baigl, D.; Williams, C. E. *Europhys. Lett.* **2005**, *71*, 938.
- (45) Beer, M.; Schmidt, M.; Muthukumar, M. *Macromolecules* **1997**, *30*, 8375.
- (46) Jeffrey, G. A. *An Introduction to Hydrogen Bonding*; Oxford University Press: New York, 1997.
- (47) Finter, C. K.; Hertz, H. G. *J. Chem. Soc., Faraday Trans. 1* **1988**, *84*, 2735.